

Z.I. Dickeson<sup>1,2</sup>, P.M. Grindrod<sup>1</sup>, J.M. Davis<sup>1</sup>, I. Crawford<sup>2</sup>, M. Balme<sup>3</sup>

<sup>1</sup> Department of Earth Sciences, Natural History Museum, London, UK.

<sup>2</sup> Department of Earth and Planetary Sciences, Birkbeck College, University of London, London, UK.

<sup>3</sup> School of Physical Sciences, The Open University, Milton Keynes, UK.

Corresponding author: Zachary Dickeson ([z.dickeson@nhm.ac.uk](mailto:z.dickeson@nhm.ac.uk))

**Key Points:**

- A detailed local study of a system of seven previously unknown palaeolakes near the dichotomy in western Arabia Terra, Mars
- High resolution topographic data aiding in identification and characterisation of palaeolakes and regional hydrological history
- Indicates a prolonged history of fluvial and lacustrine processes with palaeolakes fed by groundwater and surface accumulation

## Abstract

Hundreds of ancient palaeolake basins have been identified and catalogued on Mars, indicating the distribution and availability of liquid water as well as sites of astrobiological potential. Palaeolakes are widely distributed across the Noachian aged terrains of the southern highlands, but Arabia Terra hosts few documented palaeolakes and even fewer examples of open-basin palaeolakes. Here we present a detailed topographic and geomorphological study of a previously unknown set of seven open-basin palaeolakes adjacent to the planetary dichotomy in western Arabia Terra. High resolution topographic data were used to aid identification and characterisation of palaeolakes within subtle and irregular basins, revealing two palaeolake systems terminating at the dichotomy including a ~160 km chain of six palaeolakes connected by short valley segments. Analysis and correlation of multiple, temporally distinct palaeolake fill levels within each palaeolake basin indicate a complex and prolonged hydrological history during the Noachian. Drainage catchments and collapse features place this system in the context of regional hydrology and the history of the planetary dichotomy, showing evidence for the both groundwater sources and surface accumulation. Furthermore, the arrangement of large palaeolakes fed by far smaller palaeolakes, indicates a consistent flow of water through the system, buffered by reservoirs, rather than a catastrophic overflow of lakes cascading down through the system.

## Plain Language Summary

Evidence for hundreds of ancient lakes has been found on Mars, but these features are not distributed uniformly across the surface. The vast majority of evidence for past lakes and valleys on Mars is found within the ancient southern highlands of the planet, but even within this hemisphere there are regions with comparatively few documented ancient lakes. In this work we describe a newly discovered system of ancient lakes and river valleys which end at the geologically important boundary between the southern highlands and northern lowlands. Global catalogues of ancient lakes on Mars have generally relied on relatively low-resolution imagery and topography, but for the small area covered in this study we were able to utilise high-resolution imagery, and produce new high-resolution topographic maps. This allowed a detailed study of past water levels within each lake, analysis of numerous other features formed by lakes and rivers, and the reconstruction of a detailed sequence of events from lake filling and drainage to eventual decline and disappearance of lakes in the area.

## Introduction

The widespread occurrence of liquid water on ancient Mars is supported by evidence for hundreds of palaeolakes within the Noachian aged ( $>3.7$  Ga) southern highlands (Fassett and Head 2008b; Goudge et al. 2012; Goudge et al. 2015; Goudge et al. 2016). The global characterisation and distribution of palaeolakes has helped to constrain past climatic and hydrological conditions on Mars (Milliken, Grotzinger, and Thomson 2010; Wilson et al. 2016; Kite 2019), and to identify possible past habitable environments (Fairén et al. 2010). Studies of individual palaeolake systems have contributed to our understanding of regional hydrological histories, and although palaeolake ages generally coincide with the end-Noachian peak in global fluvial activity, many examples indicate multiple episodes of locally or regionally controlled lacustrine activity rather than a global hydrological system stable over geological timescales (Mangold and Ansan 2006; Di Achille, Hynek, and Searls 2009; Salese et al. 2016; Wilson, et al. 2016; Goudge and Fassett 2018). The continued incorporation of detailed palaeolake studies into regional and global contexts, including relationships to fluvial, groundwater and possible ocean systems, will provide a broader understanding of hydrology on Mars.

Martian palaeolakes are identified primarily upon morphological relationships between topographic basins and fluvial valley networks, and categorised as either open-basin or closed-basin. Open-basin palaeolakes are defined by outflow valleys, indicating a fill level sufficient to breach and overflow the basin (Fassett and Head 2008b; Goudge, et al. 2012). Open-basin palaeolakes are therefore the strongest evidence for standing bodies of water and are commonly associated with regionally extensive drainage systems and branching valley networks (Goudge, et al. 2016), and indicate a greater supply and duration of liquid water than a similarly sized closed-basin palaeolake which never filled to the point

of overflow. Conversely, closed-basin lakes exhibit only inlet valleys, and are typically fed by isolated, shallowly incised valleys (Goudge, et al. 2015; Goudge, et al. 2016). Most palaeolakes currently described on Mars occur within conspicuous impact craters, while a minority have been reported in tectonically controlled basins (Mangold and Ansan 2006), inter-crater basins bounded by the upraised rims and ejecta of multiple impact craters (Goudge and Fassett 2018), and other basins of undefined origin.

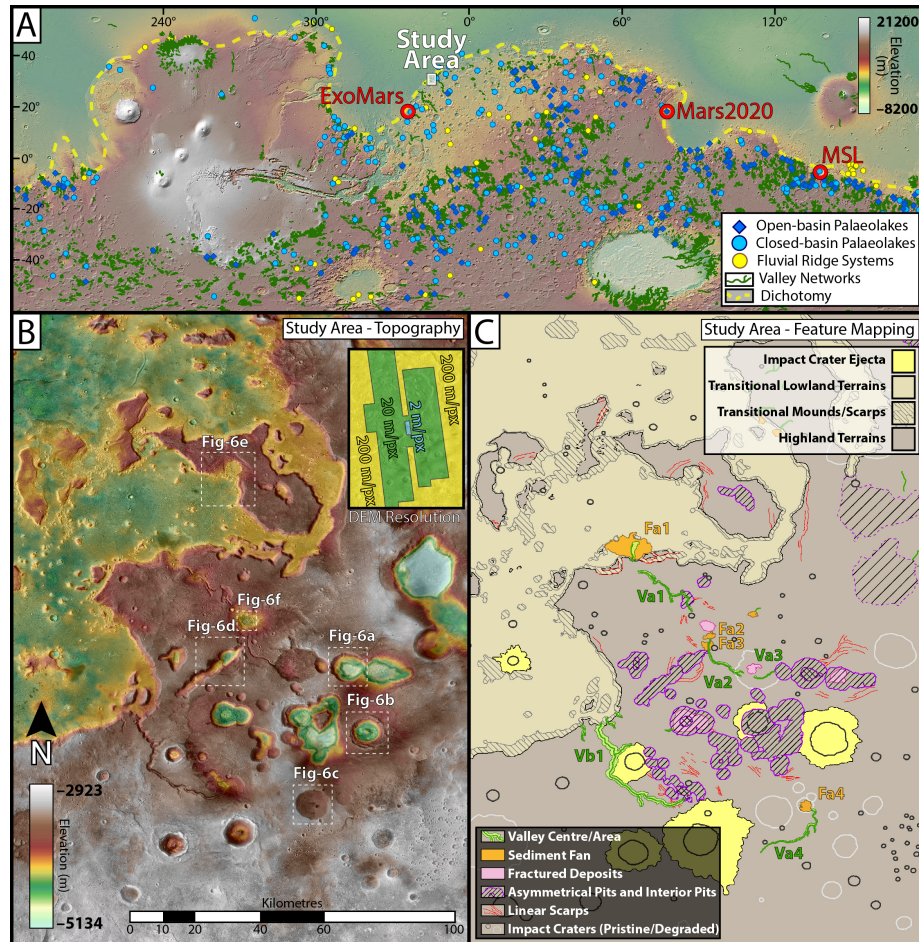


**Figure 1** – (a) Global topographic map (top) showing the study area in relation to globally catalogued open-basin (dark blue diamonds; (Goudge, et al. 2012) and closed-basin (light blue circles; Goudge, et al. 2015) palaeolakes, valley networks (green lines; Alemanno, Orofino, and Mancarella 2018), and fluvial ridge systems (yellow circles; (Dickson et al. 2020), an approximation of the planetary dichotomy (yellow dashed line), and the planned (ExoMars) and presently active (MSL & Mars2020) rover landing sites. (b) Topographic and CTX mosaic map of the study area and DEM resolutions (inset). (c) Morpho-

logical features of interest on a high resolution remapping of highland (brown) and lowland (tan) terrains (mosaic including MOLA, HRSC and CTX).

The distribution of globally catalogued martian palaeolakes (Goudge, et al. 2016; Fassett and Head 2008b) approximately correlates to that of valley networks (Hynek, Beach, and Hoke 2010; Alemanno, Orofino, and Mancarella 2018). Palaeolakes are thus almost entirely limited to the southern highlands, and many palaeolake and valley systems terminate at the edge of the northern lowlands (**Figure 1**). The processes leading to the formation and present morphology of the planetary dichotomy are not well understood (Watters, McGovern, and Irwin Iii 2007), but the dichotomy may represent the margins of an ancient hemisphere spanning ocean (Parker et al. 1986; Clifford and Parker 2001; Di Achille and Hynek 2010; Duran, Coulthard, and Baynes 2019). Regardless of the processes involved, the dichotomy appears to mark a distinct hydrological boundary, and analysis of the fluvial and lacustrine systems terminating here will be important to understanding the geological history of this planet encircling feature (Dickeson and Davis 2020).

Here, we identify and describe a group of previously undocumented palaeolakes situated adjacent to the planetary dichotomy in Arabia Terra. Making use of high-resolution digital elevation models, we analyse the topographic relationships between multiple equipotential palaeolake levels, sedimentary fans, longitudinal valley profiles, and associated geological features. Our objective is to produce a detailed history of lacustrine and fluvial processes in the area, and place these processes within the context of regional hydrology models. The fluvial and lacustrine systems which intersect or terminate at the dichotomy in this area present an additional opportunity to investigate the origin and modification of the dichotomy scarp, as well as questions regarding the existence of lowland water bodies (Di Achille and Hynek 2010).

## Study Area in Western Arabia Terra

The Arabia Terra region of the southern highlands is predominantly Noachian in age and is bounded to the north and west by the planetary dichotomy, and sits at a markedly lower elevation than the majority of the southern highlands. The region exhibits a paucity of open-basin palaeolakes (Fassett and Head 2008b; Goudge, et al. 2012) and valley networks (Carr 1995; Hynek, Beach, and Hoke 2010; Alemanno, Orofino, and Mancarella 2018), but an abundance of inverted channel systems indicative of a depositional fluvial setting (Davis et al. 2016; Williams, Moersch, and Ferguson 2018; Davis et al. 2019; Dickson, et al. 2020). In addition, the lowest areas of western Arabia Terra, near the dichotomy, are suggested as sites of significant groundwater upwelling (Fassett and Head 2008b; Andrews-Hanna et al. 2010; Salese et al. 2019), and numerous northern ocean palaeoshorelines have been mapped along this section of the dichotomy (Dickeson and Davis 2020).

Our study focuses on an area of the dichotomy marking the topographic and geo-

logical boundary between the middle Noachian highland terrains (mNh), and the Noachian-Hesperian transitional lowland terrains (HNt; (Tanaka et al. 2014). In this study, the geological units have been remapped at CTX resolution (**Figure 1**), with the contact tracing the steep scarp of the dichotomy and including large flat topped mesas to the east of the dichotomy as a part of the highland terrains (Tanaka et al. 2003; Tanaka, et al. 2014).

## Data and Methods

Geomorphological feature mapping was carried out using imaging data from NASA’s Context Camera (CTX;  $\sim 6$  m/pixel; Malin et al. 2007), with additional images from the High Resolution Imaging Science Experiment (HiRISE; 0.25–0.50 m/pixel; McEwen et al. 2007), and daytime infra-red images from the Thermal Emission Imaging System (THEMIS; 100 m/pixel; thermal; Christensen et al. 2004).

High-resolution topographic data was used in the identification and characterisation of landforms, and to define the possible hydrological relationships between mapped landforms. Topographic data was created from mosaicked CTX (20 m/pixel) and HiRISE (2 m/pixel) digital elevation models (DEMs) with approximate vertical precisions of  $<8$  m and  $<1$  m respectively (Kirk et al. 2008), and supplemented with High Resolution Stereo Camera (HRSC; 150–200 m/pixel; Neukum and Jaumann 2004) DEMs and Mars Orbital Laser Altimeter (MOLA; 456 m/pixel; Smith et al. 2001) topography data. DEMs were produced from stereo CTX and HiRISE imagery and MOLA shot heights using ISIS3 and SOCETSET software and the USGS workflow (Kirk, et al. 2008).

## Hydrological Analysis

Mapping and analysis were carried out using ESRI ArcMap software, with ‘Spatial Analyst’ and ‘Hydrology’ toolboxes used to identify equipotential surfaces, basins, and drainage catchments. Palaeolake basins were defined by equipotential surfaces within closed topographic basins at the elevations of outlet valley heads (Fassett and Head 2008b; Goudge, et al. 2012). This was achieved by generating contours at 10 m intervals, and selecting the highest closed contour at each valley head, thus defining an equipotential surface nearly overflowing the basin through the outlet valley which we refer to as the ‘valley overflow’ (VO) level (**Figure 2**). We expanded on this logic to identify up to two additional palaeolake levels within each basin: (1) a higher equipotential surface identified as the highest contour with a single opening at the outlet valley which we refer to as the ‘basin overflow’ (BO) level; and (2) a lower equipotential surface defined by the lowest closed contour at the valley head which we refer to as the ‘valley extremity’ (VE) level (**Figure 2**).

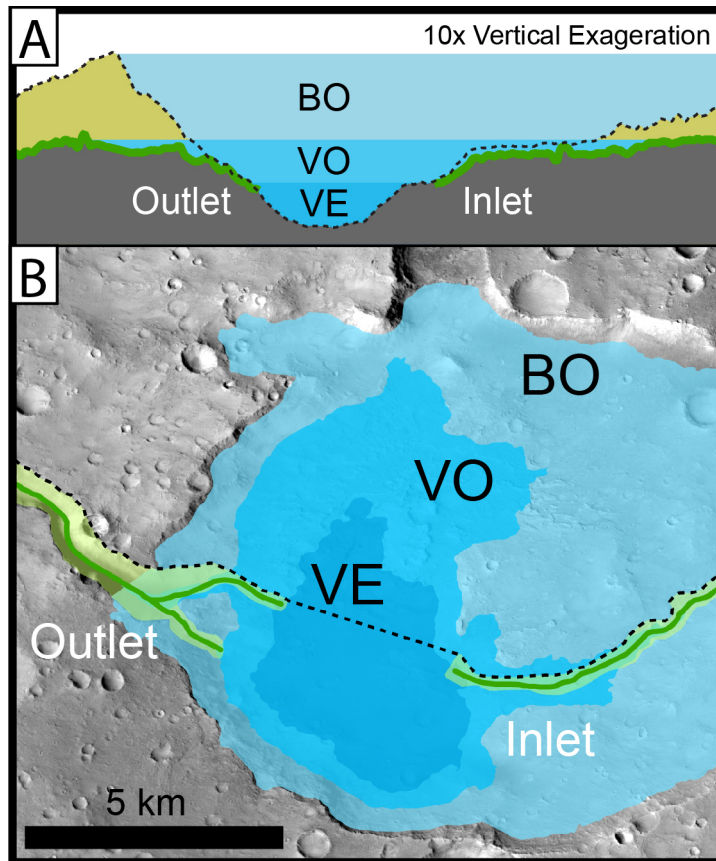


**Figure 2** - Method used to identify palaeolake basins, and equipotential surfaces. **(a)** Cross-section of topographic basin exhibiting an inlet and outlet valley, with three palaeolake levels defined by elevations of the outlet valley: basin overflow (BO), defined as the highest elevation contour within the basin with a single opening at the outlet valley; valley overflow (VO), defined as the highest closed contour intersecting the outlet valley; and valley extremity (VE), defined as the lowest contour intersected by the outlet valley. **(b)** Map-view showing the three palaeolake extents (BO, light blue; VO, blue; VE; dark blue), describing equipotential surfaces defined by the elevations observed at the outlet valley.

Drainage catchments were produced using the ArcMap 'Hydrology' toolbox on a mosaicked topographic dataset of CTX and MOLA DEMs encompassing the wider highlands region. The 'Fill' tool was used to generate a topography with no local sinks. This preparatory step negates the influence of small sinks and noise in the topographic data to produce an idealised drainage catchment, which is necessarily exaggerated as all sinks are filled regardless of depth, age, or origin. This filled topography becomes the basis for production of flow direction and flow accumulation rasters, with pour points manually selected at locations

of significant flow accumulation. Drainage catchments were then calculated using the ‘Watershed’ tool, which outputs the total upland area which would contribute surface runoff for each pour point.

## Observations and Results

In this section, we describe the morphological features mapped in this work (**Figure 1c**). Valleys (3.1) and sediment fans (3.2) represent the best evidence for liquid water in the study area, and are analysed in detail to identify and define palaeolake basins and levels (3.3). Hydrological sources and sinks are analysed in relation to highland drainage catchments, and basins within the lowlands respectively (3.4). The final sub-sections describe additional morphological features observed within the study area (3.5), and the relationships of these features to mapped valleys and palaeolakes (3.6).

### Fluvial Valleys

Incised valleys were identified and mapped on CTX imagery, with valley centrelines following the lowest elevation along the valley floor, and valley sides mapped to ascertain width and incision depth. Our analysis focused on the five longest valleys in the study area, ranging from 7.5 km to 47 km in length, and numbered from the dichotomy in order of increasing elevation (**Figure 3**). A few short (<6.6 km) tributary valleys are also present, but do not represent significant branching networks. The valleys are typically ‘V’ shaped in profile, with narrow, flat floors dominated by aeolian bedforms and lacking visible interior channels. The heads of all major valleys begin within closed basins in the highland terrains. The two longest and deepest valleys (Va1 and Vb1) terminate at the dichotomy, while the others (Va2–Va4) terminate within highland closed basins.

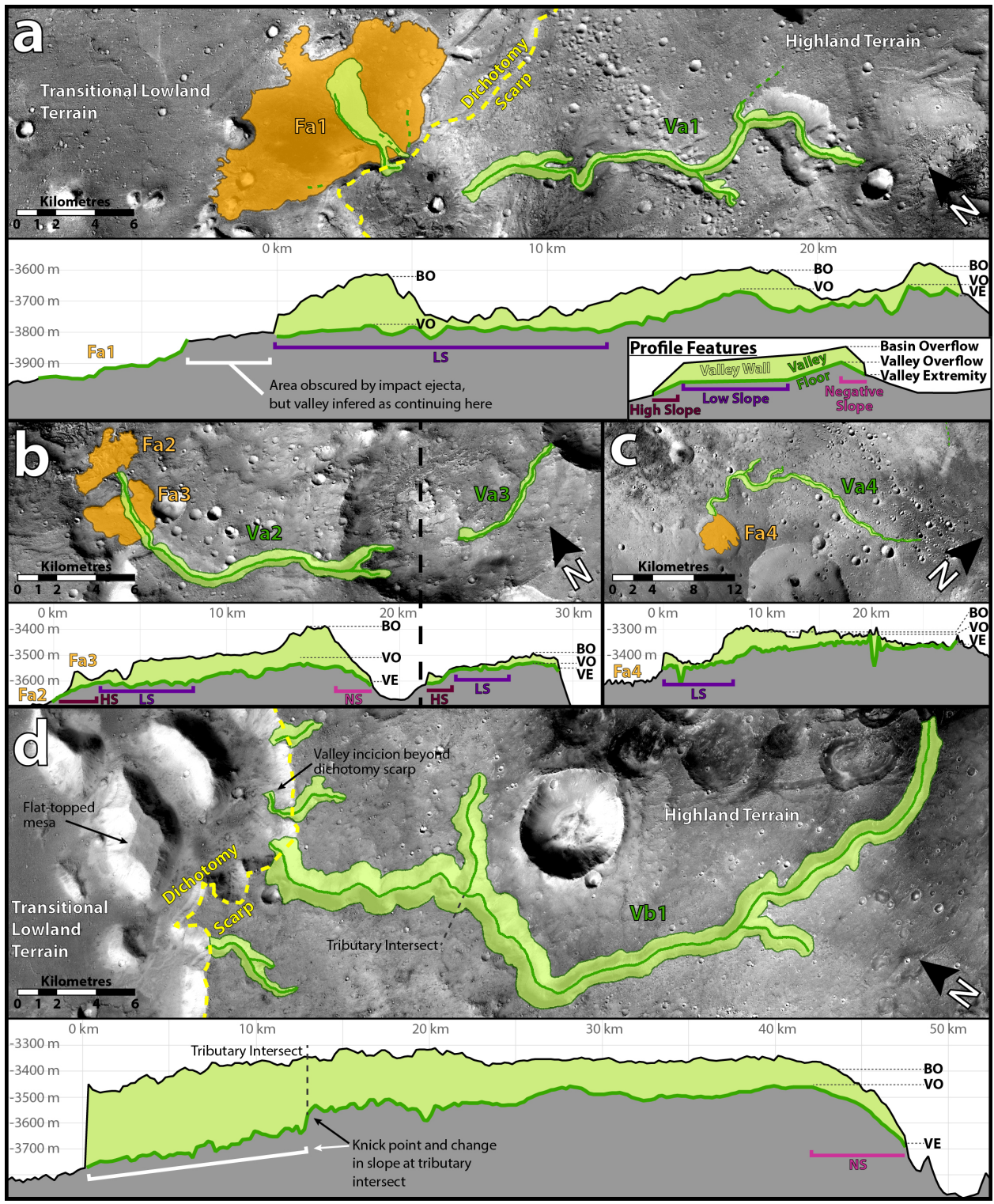


**Figure 3** – Detail images and longitudinal valley profiles for the five major valleys (dark green valley centre and light green area between valley sides), with relationships to sedimentary fans (orange areas) and the dichotomy (yellow dashed line). Slope features indicated on valley profiles include: negative slope heads (NS, pink), low slope lower reaches (LS, purple), and high slope termini (HS, dark red), with three outlet valley elevations marked where valleys transect or begin within topographic basins at: headward valley extremity (VE), valley overflow at the maximum valley floor elevation (VO), and basin overflow at the maximum valley side elevation (BO). (CTX imagery)

Longitudinal profiles show a trend of increasing incision depth from valley head to terminus, and some common trends in slope along valley length (**Figure 3**). All valleys begin with a short section of negative slope in comparison to the overall trend of the valley, meaning the elevation of the valley head is 30–260 m lower than the maximum elevation of the valley floor. In addition, the lower reaches of all (Va1–Va4) but one (Vb1) of the valleys are comparatively low slope compared to the upper reaches. Limited exceptions to this trend are short, high slope sections at the termini of valleys Va2 and Va3. Conversely, the lower reaches of Vb1 exhibit a higher slope than the upper reaches, with the transition between the two sections marked by a knickpoint coincident with the intersection of a tributary.

In close proximity to Vb1, are four short but deeply incised valleys. Three of these valleys terminate at the dichotomy, and unlike Vb1, appear incised into the dichotomy scarp (**Figure 3d**). The fourth valley nearby terminates within an asymmetrical pit in the Noachian highland terrains.

### Sediment Fans

Broad fan shaped features (Fa1–Fa4) with areal extents of 5.1–69.7 km<sup>2</sup> are observed with apexes extending from the termini of three valleys (Va1, Va2, Va4). They have lobate, distal edges marked by steep scarps and relief of ~1–100 m above surrounding terrains. Fan surfaces are heavily degraded and cratered, but are in general flat, with low and consistent downward slopes from apex to distal edge (**Figure 3**).

The largest fan (Fa1) is situated at the dichotomy at the terminus of valley Va1, although part of the valley is obscured by superposing impact craters. Distal lobes appear to deflect around raised mounds and mesas, and although the contact relationship is unclear, the fan appears to lie above transitional lowland terrains (Tanaka, et al. 2014). The fan surface is marked by numerous channels and hosts a high concentration of aeolian bedforms compared to surrounding terrains, suggesting the fan comprises fine grained, sand-grade material sourcing of the aeolian bedforms. Exposed layering is ~1 m thick, sub-horizontal and parallel.

Two fans at the terminus of valley Va3 are situated at different elevations, with the upper fan (Fa3) incised by the valley which terminates at the lower fan (Fa2)

(**Figure 3b**). The upper fan (Fa3) has a sharply-defined lobate form with steep distal edges, and sub-horizontal, parallel, layering of ~1 m thick. The lower fan (Fa2) is heavily degraded, with poorly-defined edges, and an irregular surface topography. The internal structure of Fa2 appears to be complex, with layering ~1–10 m thick, steeply dipping and possibly crosscutting with stacked lobes and channels also visible. Some areas are densely covered by aeolian bedforms, again suggesting a fine grained sedimentary material composes the fan.

The fan (Fa4) at the terminus of valley Va4 nearly covers the floor of an eroded impact crater (**Figure 3c**). The fan surface is heavily cratered, but has a general sub-horizontal upper surface, with steep distal edges, several shallow channels incised into it, and ~1 m thick, sub-horizontal, parallel bedding exposed in the walls of impact craters.

## Open Basin Palaeolakes

Seven possible palaeolake basins were identified where closed topographic basins are situated at the heads of valleys, or transected by valleys. These were numbered in order of increasing elevation from the dichotomy as follows; three (La1–La3) associated with valley Va1, one (La4) with valley Va2, one (La5) with valley Va3, one (La6) with valley Va4, and one (Lb1) with valley Vb1 (**Figure 4**). Outlet valley elevations (**Figure 3**) for valley extremity (VE), valley overflow (VO), and basin overflow (BO) were recorded, with each level interpreted and mapped as representing a possible equipotential surface and palaeolake base level. Palaeolake volumes were calculated for each of the fill levels based on the current topography (**Table 1**).

The basin overflow (BO) level represents the highest possible palaeolake level within each basin, based on a fill and spill model in which a basin filled with water and then overflowed on a topography existing before full incision of an outlet valley. The valley overflow (VO) level represents the lowest palaeolake level maintaining drainage through the outlet valley, based on overflow out of a water filled basin along the fully incised outflow valley floor. The valley extremity (VE) level, does not easily fit into a framework of basin overflow and outlet valley incision like the BO and VO levels, but has been recorded here as another possible indicator of palaeolake base level.

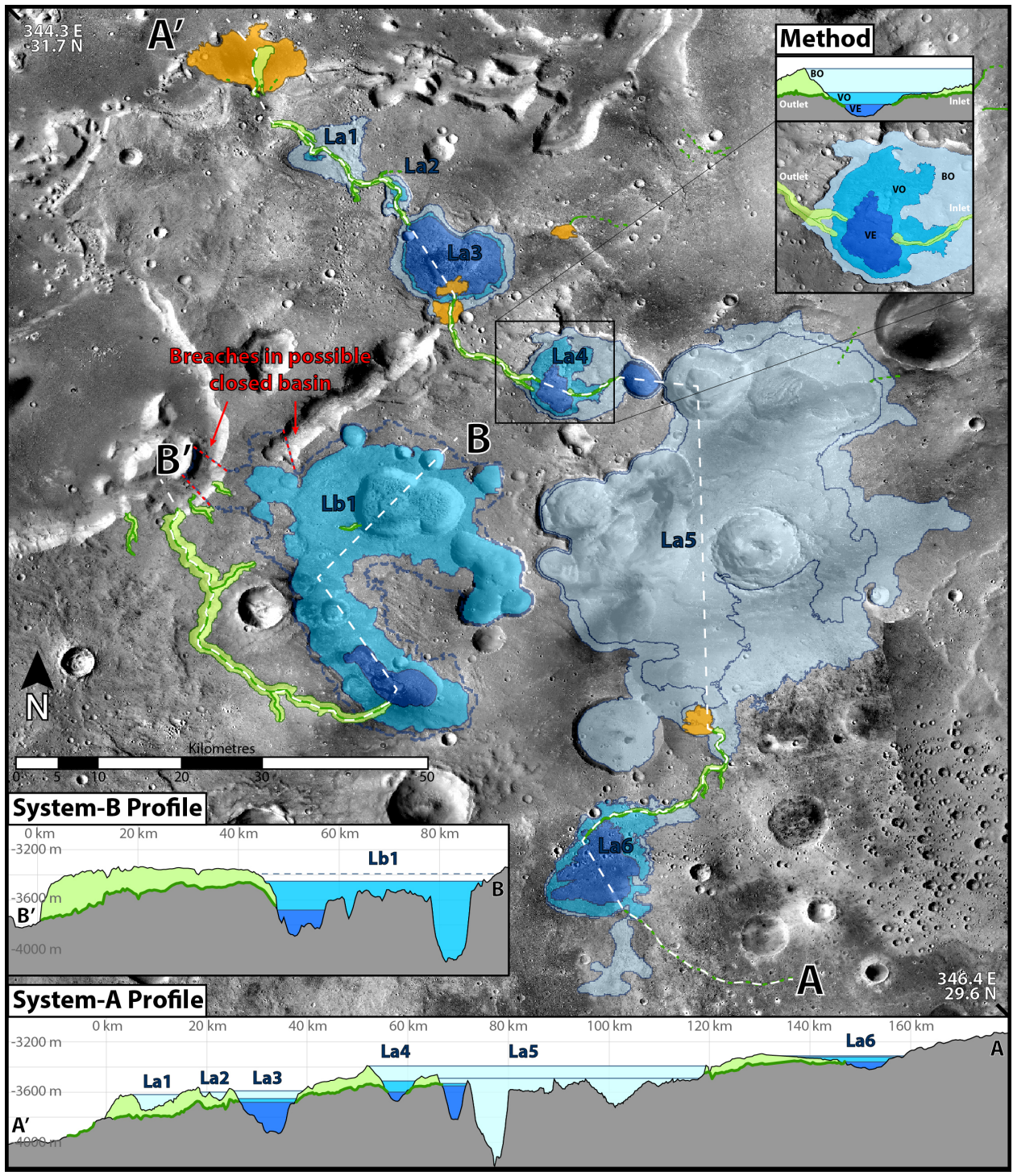


**Figure 4** – Palaeolake extents and lake/valley system profiles based on outlet valley elevations: basin overflow (BO; light blue), valley overflow (VO; mid blue), valley extremity (VE; dark blue). System-A profile displays a close correlation of palaeolake surfaces with inlet valleys and sediment fans. System-B map and profile include an approximate basin overflow level (dashed blue line), defining a nearly closed contour with the narrow areas open to the lowlands (red dashed lines). (both profiles displayed at the same scale and vertical exaggeration) (CTX imagery)

Palaeolake	Fill Level	Surface Elevation (m)	Correlation Base Level Elevations	Palaeolake Dimensions	Drainage Catchment	Inlet Valley Term. (m)	Mean Sed. Fan (m)	Mean Low Slope Reach (m)	Area (km <sup>2</sup> )	Volume (km <sup>3</sup> )	Mean Depth (V/A) (m)	Max Depth (m)	Sub-basin (km <sup>2</sup> )	Total Basin (km <sup>2</sup> )
La1	BO	-	-	-										,347
	VO	-	-	-									-	-
	VE	-	-	-									-	-
La2	BO	-	-	-										,849
	VO	-	-	-									-	-
	VE	-	-	-									-	-
La3	BO	-	-	-										,762
	VO	-	-	-									-	-
	VE	-	-	-									-	-
La4	BO	-	-	-				,691				,110		,791
	VO	-	-	-									-	-
	VE	-	-	-									-	-
La5	BO	-	-	-				,062				,010	,955	,539
	VO	-	-	-									-	-
	VE	-	-	-									-	-
La6	BO	-	-	-									,584	,584
	VO	-	-	-									-	-
	VE	-	-	-									-	-
Lb1	BO	-	-	-									,303	-
	VO	-	-	-									-	-
	VE	-	-	-									-	-

**Table 1** – Palaeolake surface elevations and dimensions for each of the three outlet-defined fill levels (BO, VO, VE) within each of the seven palaeolake basins (La1-La6, Lb1). Drainage catchment areas are shown for individual palaeolake basins and cumulatively for palaeolakes in the system-A chain.

## Highland Drainage Catchments and Lowland Sinks

Drainage catchments were calculated on a topography with all local sinks filled to determine the maximum extent of highland areas where accumulated surface water could drain into the northern lowlands (**Figure 5**). Two drainage end points were chosen where valleys Va1 and Vb1 terminate at the dichotomy, describing two drainage basins, 'A' & 'B' respectively, separated by a drainage divide. Drainage catchment 'A' has an area of 69,404 km<sup>2</sup> and extends south nearly to Mawrth Vallis. In contrast, the area of drainage catchment 'B' is an order of magnitude smaller at 3,393 km<sup>2</sup>, and only extends a maximum of ~65 km from palaeolake Lb1. Most of the palaeolakes identified in this work fall within catchment 'A' (La1–La6), and only one within catchment 'B' (Lb1). The drainage divide runs between the narrow (<2 km) raised area between palaeolakes La5 and Lb1, the two largest in the study area, indicating no surface connection between these two water bodies. Drainage sub-basins were calculated for each of the identified palaeolakes, and cumulative catchment areas calculated with higher sub-basins contributing to progressively lower sub-basins (**Table 1**).

Both drainage systems 'A' and 'B' terminate at the planetary dichotomy, at an elevation defining a basin encompassing the entire northern lowlands. Locally however, the area surrounding the valley termini defines a nearly closed basin with only limited lower elevation gaps between flat topped mesas and mounds (**Figure 5**). If the terminal fan (Fa1) associated with this valley (Va1) is a delta, it would be indicative of standing bodies of water when they formed. The contour at the same height as the mean elevation of fan Fa1 is -3940 m, defining a possible basin with a total perimeter of ~408 km, which is closed along 99% of its length, with the maximum gap to lower elevation areas being 2.7 km. The maximum elevation of fan Fa1 is -3778 m, defining a wider basin with a perimeter of ~499 km, which is still closed along 87% of its length, with the widest gap to lower elevation areas being 15 km.

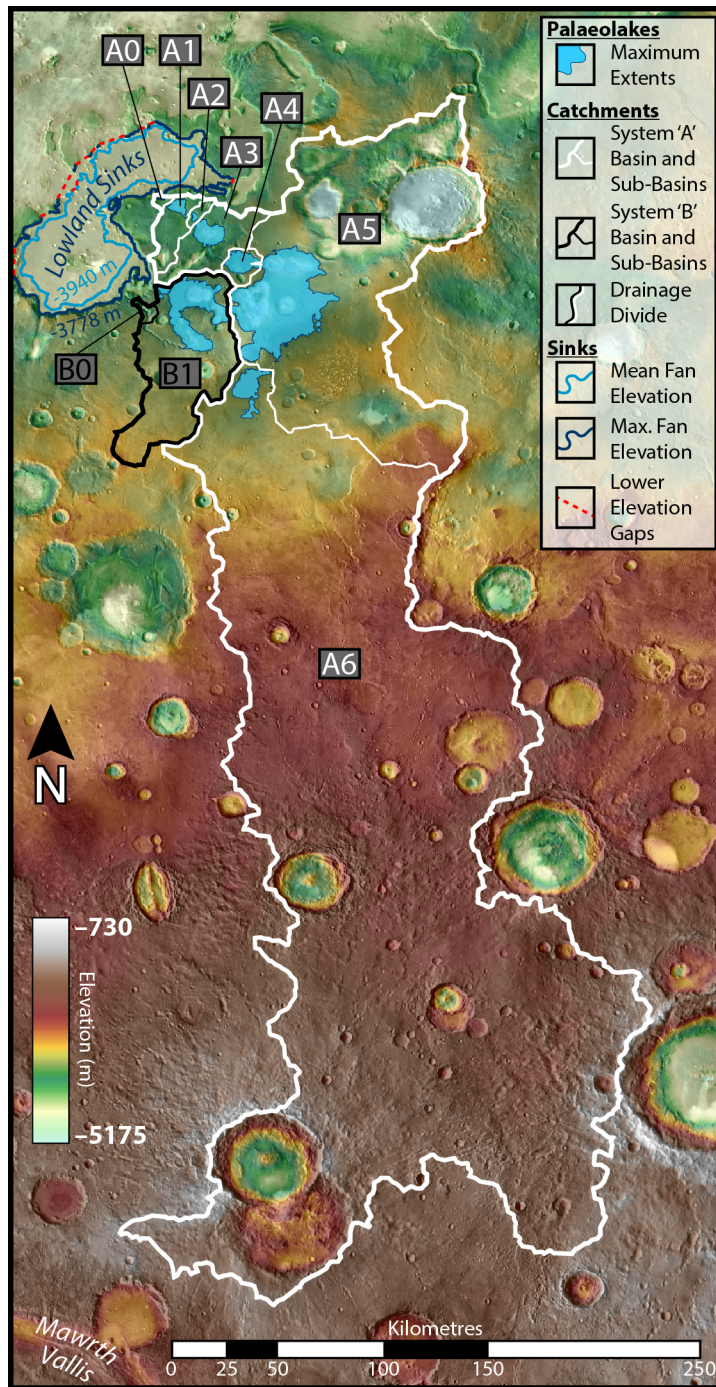


Figure 5 – Highland drainage catchments for palaeolake systems 'A' (white

borders) and ‘B’ (black borders) terminating at the dichotomy, showing numbered sub-basins (thinner white and black borders respectively) for each individual palaeolake (light blue areas). Possible base levels within lowland sinks are shown for the mean (light blue dashed line) and maximum (dark blue dashed line) elevations of sediment fan Fa1, indicating basins open to the entire northern lowlands but only breached at narrow areas between flat topped mesas (red dashed lines). (Background is THEMIS daytime mosaic overlain on MOLA hillshade)

## Associated Morphological Features

### Basin Morphology

Impact craters form ubiquitous topographic basins across the surface of Mars, and catalogued martian palaeolakes are often hosted within these conspicuous features (Cabrol and Grin 1999; Goudge, et al. 2015). The irregular palaeolake geometries exhibited in this study suggest a variety of basin origins, and here we describe four morphologically defined basin types: (1) pristine impact craters, (2) filled/degraded impact craters, (3) asymmetrical pits, and (4) undefined basins. (**Figure 6**). These basins are assessed in terms of relationship and influence on mapped palaeolake areas, depths and volumes.

Pristine impact craters (**Figure 6b**) exhibit raised rims, steep interior sides, a uniform depth to diameter ratio, and often have raised central peaks and ejecta blankets. These craters are thought to postdate the palaeolakes, but only the two largest palaeolakes (La5 and Lb1) are superposed by large pristine impact craters or their ejecta, and they do not appear to greatly influence measurements of palaeolake dimensions. Filled, eroded, or otherwise degraded impact craters (**Figure 6c**) are typically shallow and flat floored, with no uniform depth to diameter ratio. Palaeolake basin La4 is situated entirely within a degraded crater, and the southern edge of palaeolake basin La5 is partially defined by overlapping degraded craters.

Asymmetrical pits (**Figure 6a,d**) are limited to the Noachian highland terrains and concentrated near the mapped palaeolakes. Small asymmetrical pits are bowl-shaped in profile and circular or semi-circular in plan-view. Larger examples appear to be composed of conjoined smaller pits, and are typically asymmetrical with cusped or scalloped edges and narrow curvilinear interior ridges. Pit edges are sharply-defined, without raised rims, and have relatively consistent depths with no uniform depth to diameter ratio. Some asymmetrical pits also host secondary interior pits which are morphologically similar to the primary pits. Palaeolake La2 is situated completely within an asymmetrical pit, and although limited lengths of other palaeolake edges (La4, La5, Lb1) are defined by asymmetrical pits, the majority are situated fully within palaeolake basins La5 and Lb1. Unlike pristine or degraded impact craters, asymmetrical pits appear to be the result of more complex formation processes, and appear to be one of the youngest features in the study area, forming abrupt, steep,

sharp edges where they intersect degraded impact craters, valleys (Va3), and the ejecta of pristine impact craters (**Figure 1c**). Given the significant depth of these features, the calculated water-holding volumes in basins with asymmetrical pits (La4, La5, and Lb1) may be gross overestimates if the pits formed subsequent to palaeolakes.

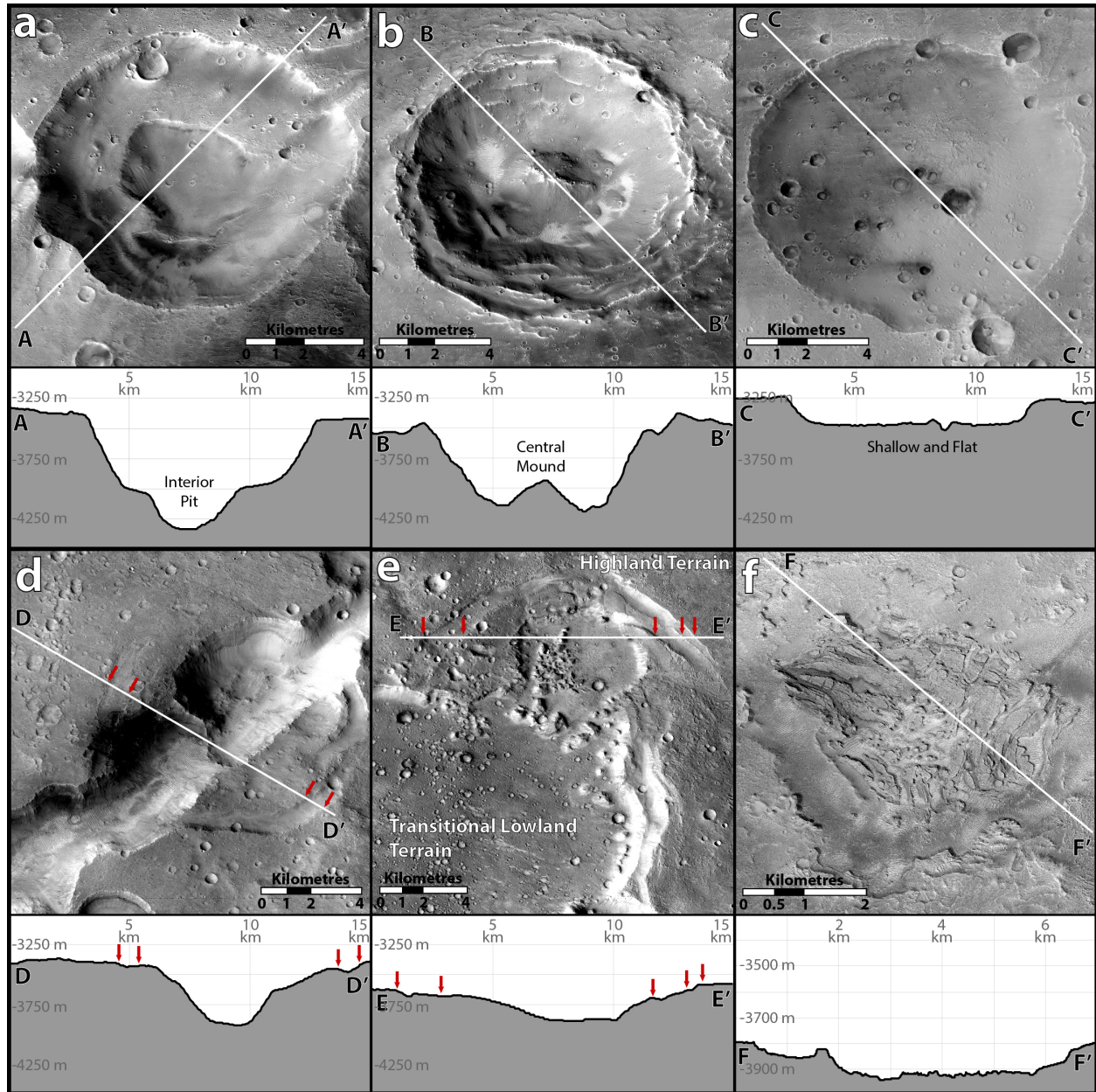


**Figure 6** – Morphological features associated with palaeolake basins, in plan-view and profile: (a) asymmetrical pit displaying no raised rim, steep sides, and a secondary interior pit, (b) pristine impact crater displaying raised rim, steep sides, and central mound, (c) degraded impact crater displaying slight raised rim and shallow flat floor, (d) an elongate asymmetrical pit apparently formed from coalesced circular and sub-circular pits, and surrounded by linear scarps (red arrows), (e) linear scarps (red arrows) arranged along the edge of a large flat-topped mesa, (f) fractured basin floor deposits. North is up in all images. Profiles for a-e shown at the same vertical exaggeration. All images from CTX.

Besides the palaeolakes hosted within impact craters (La4) and asymmetrical pits (La2), and the limited sections of palaeolake extents partially defined by these features, the majority of palaeolakes (La1, La3, La5, La6 and Lb1) identified in this study are hosted within relatively shallow, irregular shaped basins without conspicuous edges or easily definable origins.

Basin floor deposits (**Figure 6f**) with a fractured appearance are observed within deeper areas of palaeolake basins La3, La4, La5 & Lb1 (**Figure 1c**). These deposits are characterised by raised blocks (~150–500 m) separated by steep-sided, flat-floored fissures. The sides of fractured blocks reveal fine (~1–10 m) layering, and the surfaces of some blocks display a corrugated appearance, with the orientation of minor fractures apparently influenced by the orientation of ripples in the bedrock surface.

### Dichotomy Scarp

The dichotomy scarp marks the sharp contrast between the highland and lowland terrains, and has a prominence of up to ~600 m in the study area, reducing to ~300 m and ~100 m at the terminus of valleys Vb1 and Va1 respectively. In profile the dichotomy scarp is very steep, and in planform displays a cusped geometry similar to the asymmetrical pits. These attributes are also shared by the scarps surrounding large flat-topped mesas (**Figure 6e**), and may indicate a common formational origin for all three features.

The dichotomy scarp where intersected by valley Va1 (-3900 m) is low and gently sloping, and sediment fan Fa1 appears to have formed over lowland deposits (**Figure 3a**). In contrast, valley Vb1 (-3800 m) terminates abruptly at the dichotomy with no sediment fan and without extending beyond the high steep scarp in this area (**Figure 3d**). These relationships suggest that in the area of valley Va1 the dichotomy scarp predates fluvial activity, but that in the area of valley Vb1 alteration (e.g., erosional retreat) of the dichotomy scarp has occurred which postdates fluvial activity.

### Linear Scarps and Troughs

Linear scarps with heights of ~1–100 m are observed within the Noachian highland terrains, commonly as pairs and sets arranged in parallel, with depressed troughs between inward dropping scarps (e.g. similar to a graben structure), or

stepwise with scarps set progressively lower. In no cases do the low sides of parallel scarps face outwards to form a raised interior section (such as in a horst). Linear scarps are concentrated near the margins of asymmetrical pits (**Figure 6d**), the dichotomy scarp and the edges of large flat-topped mesas (**Figure 6e**). They often mirror the geometry of these larger scarps, as inwardly depressed elliptical rings around asymmetrical pits, or parallel to the dichotomy and mesa edges, possibly indicating a linked origin or formation process.

## Relative Age Relationships

Determination of absolute ages for martian valley networks is difficult due to the small and narrow areal extents available for crater counting. A method for buffered crater counting has been successful in dating large valley networks (Fassett and Head 2008a), but the relatively short valleys (<47 km) in our study preclude this as an option, and no valleys or palaeolakes coincide with superposing impact ejecta blankets large enough for crater counting. As such, this work is limited to the relative age relationships between features, and inferences based on the age of the terrains which host them.

All of the valleys within this study are incised into Noachian aged highland terrains, with some valleys (Va2 – Va4) and sediment fans (Fa4) clearly overlying degraded impact craters. Although valley Vb1 appears to be either incised through or partially covered by the ejecta of a ~5 km impact crater there are no unambiguous relationships between fluvial features and large pristine impact craters (**Figure 1c**). The approximate age of valleys, sediment fans and palaeolakes is therefore presumed as matching the Noachian peak in fluvial activity, postdating ancient degraded impact craters and predating pristine impact craters. However, a younger age cannot be excluded.

## Discussion

### Analysis of Palaeolakes and Valleys

#### Palaeolake Overflow and Valley Incision

Basin overflow (BO) and valley overflow (VO) levels are interpreted as marking temporally distinct base levels at the initiation and cessation of drainage out of each palaeolake basin, with an interceding period of falling palaeolake levels driven by outlet valley incision.

Basin overflow levels represent the highest possible base levels and extents of palaeolakes at the initiation of basin overflow immediately prior to outlet valley incision, and have been calculated similarly to other studies (Goudge and Fassett 2018; Salese et al. 2020). Basin overflow levels within catchment ‘A’ (La1–La6) all define basins with the lowest basin margin coincident with an outflow valley (**Figure 4**), supporting a model of outlet valley incision initiated as higher basins filled and spilled over to fill lower basins, in contrast to an alternate

basin breaching model of sapping erosion and upstream propagation of valley heads from lower to higher basins.

In contrast, the basin overflow level in palaeolake basin Lb1 does not describe a closed basin, and the contour at this elevation (-3360 m) is open to the northern lowlands and inconsistent with a palaeolake on the current topography. As a maximum palaeolake level cannot be determined with certainty, we considered the -3390 m contour to be a useful approximation of palaeolake level prior to outlet valley incision, defining a nearly closed basin only broken at the dichotomy scarp and by asymmetrical pits which appear to postdate palaeolakes and valleys. The outlet valley (Vb1) of basin Lb1 is also in close proximity to three large craters, and the valley sides may have been raised by ejecta postdating valley incision.

Incision of outlet valleys progressively lowered the elevation of valley heads, in turn lowering palaeolake base levels, reducing palaeolake extents and allowing inlet valleys to incise further and lower into palaeolake basins (**Figure 4**). Valley incision may have progressed gradually as a result of continuous drainage, or punctuated by multiple discrete overspill events. However, the arrangement of large palaeolakes in the middle of the system (La5) fed by smaller upstream palaeolakes (La6), suggests a constant flow through the system rather than the filling and breach of a single large source basin. Valley incision and erosion rates have been calculated for other valley systems on Mars (Rosenberg and Head 2015), but are limited due to a lack of understanding of the lithology and poorly constrained rheology of the host rock, and were therefore not quantified in this study.

Outlet valley incision continued to reduce palaeolake extent until the input flux of water to each lake was no longer sufficient to overcome loss of water through infiltration and evaporation and hence the water level became insufficient to overflow the basin. The valley overflow (VO) levels represent the open-basin palaeolakes at the cessation of outlet valley incision. If at this time the inlet water flux remained similar to the rate of loss of water through infiltration and evaporation, then these basin would have become closed-basin lakes instead.

### **Correlation of Palaeolake Base Levels**

Martian oceans in the northern lowlands and closed basin palaeolakes, which by definition lack outlet valleys, are often identified based on observations of valley terminations, channel topography, deltas, palaeoshorelines, and basin floor deposits (Di Achille and Hynek 2010; Goudge, et al. 2015; Goudge and Fassett 2018; Dickeson and Davis 2020). In isolation these diverse features may not conclusively indicate a standing body of water, but constitute corroborative evidence where observed within outlet-valley defined palaeolake basins, and where correlating with or situated between basin and valley overflow levels (**Table 1**).

The observed location and elevation of valley terminations can result from cessation of incision at a standing body of water, or due to changes in lithology,

slope, or subsequent destruction or burial of a valley. The three major valleys (Va2–Va4) which terminate within palaeolake basins (La3–La5) terminate on slopes which continue basinward and do not coincide with any obvious lithological changes. Two valley terminations (Va2 & Va3) correlate closely to valley extremity levels (La3, +3 m; La4, -7 m), and although valley Va4 is poorly correlated to a basin overflow level (La5, +45 m) the elevation (-3445 m) falls between the basin overflow levels of La4 (-3390 m) and La5 (-3490 m).

Sediment fans are difficult to characterise as one or other of sub-areal alluvial fans or deltas, but the flat surfaces and steep distal edges of fans in this study support interpretation as possible deltas (Di Achille and Hynek 2010; Fawdon et al. 2018). The mean elevation of two possible deltas (Fa2 & Fa4) correlate well to basin overflow levels (La3, -4 m; La5, -7 m), and that of fan Fa3 is situated somewhat below the valley extremity level (La3, -29 m).

A stable base level at the terminus of an inlet valley can affect the valleys longitudinal profile, resulting in a low slope in the valleys lower reaches (Langbein and Leopold 1964), as observed elsewhere on Mars (Duran, Coulthard, and Baynes 2019). The mean elevations of low-slope lower-reaches for palaeolake inlet valleys (La2–La4) do not correlate well to basin overflow (La3, -18 m; La4, -47 m) or valley overflow levels (La4, -41 m), but do fall below outlet-defined palaeolake levels in each basin.

### Negative Slope Outlet Valleys

Unlike the basin overflow (BO) and valley overflow (VO) levels, the valley extremity (VE) levels do not easily fit into a framework of palaeolake overflow and drainage. In a draining palaeolake, the VE level would be expected to match the VO level, as the highest point of the outlet valley would be at the valley head. Instead, every valley extremity level is lower than the corresponding valley overflow level, particularly within basins La4 (60 m) and Lb1 (260 m). Although basin La2 lacks a valley extremity level, the valley floor within the basin is ~70 m lower than the valley overflow level (**Figure 3**). At the edges of these palaeolake basins the valley slope is negative relative to the overall trend of the valley, and here we consider three possible scenarios accounting for this observation.

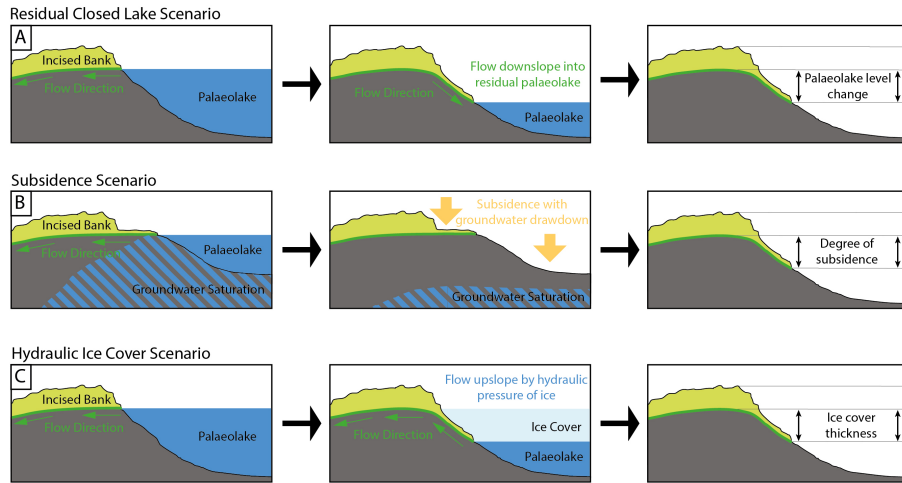


**Figure 7** – Scenarios accounting for the formation of observed negative slope outlet valleys. **(a)** Residual closed lake; in which a short and shallow section of valley is incised into the basin at a time after base level has fallen to form a closed basin palaeolake. **(b)** Subsidence; in which the outlet valley is formed by drainage out of the palaeolake followed by subsidence, perhaps driven by groundwater drawdown within the basin. **(c)** Hydraulic ice cover; flow up and out of the basin is facilitated by significant pressure resulting from ice coverage.

Valley extremity levels may represent the base levels of closed basin palaeolakes, with negative slope outlet valleys formed by a basinward flow of surfacing groundwater or minimal surface accumulation after cessation of palaeolake drainage through the system (**Figure 7a**). This scenario could also explain the similarly steep and shallowly incised inlet valley terminations which correlate to outlet valley extremity levels within basins La3 and La4.

Alternatively, subsidence in basins subject to significant desiccation or groundwater drawdown has been recorded in terrestrial basins on historical and geological time scales (Ireland, Poland, and Riley 1984). In this scenario, negative slope outlet valleys apparent on the current topography would have formed during palaeolake drainage, but would have been later lowered by subsidence of the basin (**Figure 7b**). The basinward dropping linear scarps arranged around the edge of palaeolake basin La3 could be further indications of this process (**Figure 1c**).

A final consideration is that negative slope valleys formed by upward flow facilitated by the pressure of an overlying ice sheet (**c**), as observed in subglacial lakes on Earth (Cook and Swift 2012). Ice coverage would have profound implications on the interpretation of fluvial and lacustrine systems in this study and across the region, and other studies postulate periods of extensive ice coverage in the southern highlands (Baker et al. 1991; Head and Marchant 2014; Palumbo, Head, and Wordsworth 2018). We observed no glacial or sub-glacial

landforms in our study, but this scenario should be revisited if further evidence of regional ice sheets comes to light.

## Nature of the Dichotomy Margin

Globally mapped shorelines of postulated lowland oceans are generally poorly constrained spatially or by elevation (Sholes et al. 2021; Dickeson and Davis 2020). However, within Arabia Terra potential shorelines closely follow the dichotomy, accounting for a relatively narrow range of elevations within our study area; one transects palaeolake La1 (−3770 m; (Parker, Saunders, and Schneeberger 1989), three approximately follow the dichotomy near the termination of valley Va1 (∼−3900 - −3600 m; (Clifford and Parker 2001; Carr and Head 2003; Webb 2004), and a further three are traced through the lowlands ∼60-70 km NNW of Fa1 (∼−4000 m; (Parker, Saunders, and Schneeberger 1989; Carr and Head 2003; Webb 2004).

Valley terminations and possible deltas have also been interpreted as representing the global margin and base level of a hemisphere spanning ocean on Mars (ocean surface level -2540 m; (Di Achille and Hynek 2010), and detailed analysis of individual deltas has produced similar outcomes (ocean surface level, -2500 m; (Fawdon, et al. 2018). In contrast, topographic analysis of possible deltas in other regions indicate a number of lowland palaeolakes or small seas adjacent to the dichotomy, rather than a hemisphere spanning ocean (Rivera-Hernández and Palucis 2019; García-Arnay and Gutiérrez 2020).

Situated at the dichotomy, sediment fan Fa1 (−3940 m), along with the termination (−3815 m) and low slope lower reaches (−3791 m) of valley Va1 constitute possible base levels within the northern lowlands which correlate well to global shorelines mapped along the dichotomy, but are a poor match to delta defined ocean base levels. On the current topography the lowland base levels in our study would indicate a water body filling the entire northern lowlands, but could instead indicate a palaeolake limited to a local lowland basin as illustrated in **Figure 5**.

The morphological similarities between the dichotomy scarp, mesa scarps, and the sides of asymmetrical pits (**Figure 6**) suggest a possible common origin, consistent with collapse postdating fluvial and lacustrine activity. A similar origin has also been proposed for mesas in the Oxia Planum area to the southeast of this study (McNeil et al. 2021). Collapse along the edges of flat topped mesas would indicate a closed-basin palaeolake in the lowlands, and collapse along the dichotomy and within asymmetrical pits would explain the lack of a sediment fan or clear termination where valley Vb1 intersects the dichotomy, and the open contour for palaeolake Lb1. Significant changes in the morphology and position of the dichotomy since the Noachian would have important implications for our understanding of the formation of the dichotomy and the mapping of lowland ocean shorelines (Dickeson and Davis 2020).

Valley Vb1 displays a pronounced knickpoint corresponding to the intersection

of a tributary valley (**Figure 3**). This profile may indicate a significant lowering of base level within the northern lowlands basin, and more recent drainage forming the knickpoint and tributary. Similar knickpoints elsewhere on Mars have been interpreted as representing multiple episodes of fluvial activity and/or changes in base level (Goudge and Fassett 2018; Duran, Coulthard, and Baynes 2019).

## Regional Hydrology and Martian Palaeolakes

Global palaeolake catalogues have so far identified only one open-basin palaeolake in western Arabia Terra (Fassett and Head 2008b; Goudge, et al. 2012), but local studies to the north and south of our study have identified additional examples (Wilson, et al. 2016; Fawdon et al. 2021). The seven open-basin palaeolakes in this work are therefore significant in further characterising the style, distribution, and frequency of lacustrine processes in the region, and add to the broader understanding of lacustrine systems on Mars.

The palaeolakes and valleys discussed in this work are situated within Noachian highland terrains (Tanaka, et al. 2014), but this only affords an upper limit to their age. The peak in fluvial and lacustrine processes on Mars is generally agreed to have occurred during the Noachian to early Hesperian (Fassett and Head 2008b; Goudge, et al. 2012; Goudge, et al. 2016), although some studies suggest palaeolakes may have been active as late as the middle Amazonian (Wilson, et al. 2016). One global study (Goudge, et al. 2016) associates palaeolakes fed by extensive valley networks with an early period of formation prior to 3.7 Ga, and those fed by limited valleys with a later period of reduced hydrological activity during the Hesperian or Amazonian (<3.7 Ga). The palaeolakes in our study are difficult to categorise by these criteria, as they constitute a long chain of palaeolakes, yet are only connected by short, non-branching valleys. However, the greater supply and duration of liquid water required to fill open-basin palaeolakes, and the evidence supporting continuous flow through the system rather than a single catastrophic overflow, leads us to conclude that the palaeolake systems described in this work fit with the period of palaeolake activity prior to 3.7 Ga.

The palaeolakes in this study are slightly smaller and shallower than the mean of globally catalogued open-basin palaeolakes, but well within the global range (Fassett and Head 2008b). A high ratio of palaeolake volume to catchment area has been highlighted as an indication of filling by groundwater rather than surface runoff, but only for palaeolakes not fed by other palaeolakes as part of a chain (Fassett and Head 2008b). In our study a comparison is therefore only useful for palaeolakes Lb1 and La6 which are not fed by higher palaeolakes, and La5 which is only fed by a much smaller palaeolake (La6). Of these three palaeolakes, only Lb1 displays a volume:catchment ratio indicative of groundwater as the dominant water source. Furthermore, palaeolakes Lb1 and La6 do not have inlet valleys, and although this is another possible indication of filling by groundwater, other studies have shown that significant accumulation and

surface flow is possible with little to no channelization (Lamb et al. 2008).

Western Arabia Terra has been identified as a region of significant groundwater upwelling, particularly in areas adjacent to the dichotomy (Andrews-Hanna, et al. 2010), and this process was probably important in filling palaeolakes across the region (Fassett and Head 2008b). Overflow of the palaeolakes in our study appears to have been primarily driven by surface drainage through the system, although it is possible that upwelling groundwater played a role in the original filling of these basins, with earlier palaeolakes existing as unconnected, closed-basin palaeolakes, only requiring minimal additional input to become sufficiently full to breach and drain. However, to identify evidence of such lakes is beyond the scope of the present study.

Fractured basin floor deposits as observed within some palaeolakes in our study area are a feature common to many martian palaeolakes, and are described within the deepest palaeolake basins in an area to the north of our study (Wilson, et al. 2016), with larger scale fractured floor deposits found in association with many other palaeolakes on Mars (Goudge, et al. 2012). In Xanthe Terra, to the south of our study, these features are interpreted as having formed by rapid discharge and eventual groundwater depletion within closed palaeolake basins (Sato, Kurita, and Baratoux 2010). Additionally, the rippled surfaces of some fractured floor deposits in our study appear analogous to the ‘washboard’ terrains observed in Gale crater, where they are interpreted as aeolian dunes preserved beneath closed-basin palaeolake deposits (Milliken et al. 2014; Favaro et al. 2021). The Mars2020 mission is the in early phases of science operations in Jezero crater, but will hopefully soon provide examples of sedimentation within an open-basin palaeolake, and provide a further opportunity to contrast the findings of our remote sensing interpretations.

## Local Hydrological and Geological Evolution

The identification of multiple palaeolake fill levels and varied morphological features in this work allows a detailed reconstruction of events, and here we interpret the sequence of hydrological and geological processes leading to the palaeolake and valley landforms observed in this region of Arabia Terra. Palaeolake basin La6 is the only basin that shows evidence consistent with filling by surface accumulation without input from other palaeolakes, and is the highest basin in the area, with the strong correlation between inlet and outlet valleys indicating that all the other palaeolakes, other than Lb1, were fed by inlet drainage ultimately originating from palaeolake La6. The fact that the volume of palaeolake La6 is so much smaller than lakes further down the system indicates that there was consistent flow through the system buffered by basin reservoirs, rather than a single filling and spilling event from top to bottom.

In system ‘A’, a continuous chain of valleys and lakes drained water and sediment from the highlands to the lowlands, with palaeolakes cascading down through the system from basin La6, draining through valley Va4 to form sediment fan

Fa4 and fill basin La4, draining through valley Va3 to form sediment fan Fa3 and fill basin La3, and then draining through valley Va1 (**Figure 8e**). Valley Va1 was originally three short isolated sections, with the first draining from La3 to fill basin La2, a second section draining La2 to fill basin La1, and a third section draining La1 and terminating at the dichotomy to form sediment fan Fa1.

In system 'B', the limited drainage catchment and lack of inlet valleys suggest that basin Lb1 was filled by groundwater, and then drained through valley Vb1 to debouch into the lowlands (**Figure 8b**). The close proximity and correlated elevations of basin overflow levels in La4 and Lb1 could also indicate groundwater communication between the two systems, with Lb1 partially fed by groundwater from the more extensive system 'A'.

Continued drainage through both systems led to progressively lower palaeolake levels caused by outlet valley incision lowering the elevation of the outlet spillway (**Figure 8c,f**). Significant outlet valley incision resulted in complete drainage of the palaeolakes in basins La1 and La2, allowing inlet valleys to incise the previously submerged lake floors to become one continuous valley (Va1). Incision of valley Va1 also caused base level to fall in basin La3, allowing inlet valley Va2 to incise down and through sediment fan Fa3, with the apex of a new sediment fan (Fa2) forming basinward at the new termination of valley Va2 (**Figure 8f**). Incision of valley Va2 caused a base level fall and significant reduction in lake extent within palaeolake La4, with the basin fed by a newly formed valley (Va3) draining from palaeolake La5 and incising across the previously submerged palaeolake floor. The late exposure of Va3 and sections of La1 in this area would also explain the relatively shallow incision depth of these valleys.

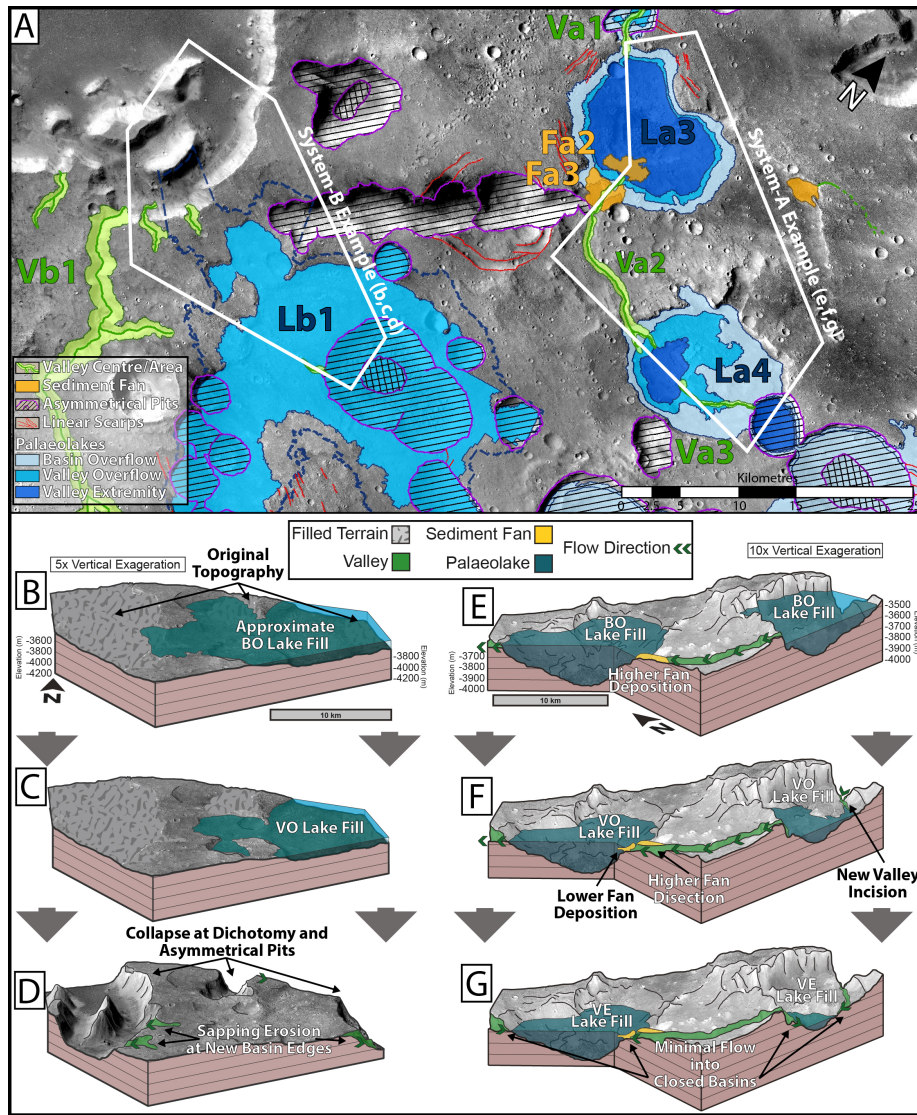


**Figure 8** – (a) Representative areas of system ‘A’ including palaeolake basins La3 and La4; and system ‘B’ including palaeolake basin Lb1 and the dichotomy scarp, and chronologies of fluvial and lacustrine processes in system ‘A’ (e,f,g) and system ‘B’ (b,c,d). The top diagrams (b&e) show the highest palaeolake fill levels (BO) at the initiation of palaeolake drainage, (e) with the formation of fan Fa3 at the end of valley Va2, (b) and an approximate topography with asymmetrical pits and the dichotomy scarp filled. The middle diagrams (c&f) show reduced palaeolake levels (VO) resulting from outlet valley incision while drainage out of the basins continued. (f) Fan Fa3 was incised through by valley Va2 to form the new lower fan Fa2, and base level lowered within basin La4

so that valley Va3 began to incise across the former lake floor. The bottom diagrams (**d&g**) show the lowest palaeolake levels (VE), likely fed by ground water or minimal surface accumulation, (**d**) and the current topography resulting from the formation of asymmetrical pits and the dichotomy scarp. (CTX imagery on CTX DEM topography)

At the cessation of palaeolake overflow and drainage, palaeolakes were filled to the valley overflow level, and stable base levels in now closed basins or ephemeral palaeolakes probably likely within some basins (La3–La6, Lb1) (**Figure 8d,g**).

After drainage through the palaeolake systems had ceased, collapse within highland terrains formed asymmetrical pits and modified the scarps of the dichotomy and the margins of flat topped mesas (**Figure 8d**). The result was a topography that no longer reflected some original palaeolake volumes, and left gaps to the lowlands in the previously closed basin of Lb1 and a possible closed basin in the lowlands.

## Conclusions

High resolution CTX imagery and DEMs facilitated the discovery and characterisation of this palaeolake system, and allowed for precise calculations of palaeolake fill levels and drainage catchments. The identification of three temporally distinct palaeolake fill levels linked to different outlet valley elevations was key to understanding changes in palaeolake base level and valley incision over time, and allowed fully drained palaeolake basins to be identified. Additional analysis of longitudinal valley profiles and possible deltas strengthens the evidence for these basins having hosted lakes, and provides insight into the hydrological evolution of the area.

Significantly, these palaeolakes indicate a combination of groundwater sources and surface accumulation, supported by a climate sufficiently warm and stable for prolonged fluvial and lacustrine processes during the Noachian. The discovery of finely bedded lake deposits laid down during this potentially habitable period, which are incised though by subsequent valleys, presents an ideal site for future palaeo-climatic and astrobiological exploration.

That such a complex yet localised system has not been included in previous catalogues suggests that many other hitherto unrecognised palaeolakes may exist on Mars, and are likely to be revealed with the increased use of high resolution images and topography. Compared to crater-hosted palaeolakes which are typically deep and exhibit clearly defined edges, palaeolakes of the type described here display more subtle topographic profiles, and are likely to be underrepresented in palaeolake catalogues. Undertaking similar detailed studies on the hundreds of palaeolakes already identified in global catalogues, has the additional potential to greatly expand our knowledge of water sources, comparative regional hydrology, and further characterise the past climate of Mars.

## Acknowledgments

Funding for this project and ZID was provided by the UK Science and Technology Facilities Council grant STFC-1967420. MRB was supported by UK Space Agency grants (ST/T002913/1, ST/V001965/1, ST/R001413/1, PMG was also supported by the UK Space Agency (ST/R002827/1, ST/R002355/1) and ST/W002744/1), and MD gratefully acknowledges UK SA support (ST/R002355/1; ST/V002678/1; ST/W002566/1).

## Open Research

Primary image and topographic data used in this research can be accessed on the Mars Orbital Data Explorer of the Planetary Data System (PDS) (<https://ode.rsl.wustl.edu/mars/>) for: CTX (Malin, et al. 2007), HiRISE (McEwen, et al. 2007), and MOLA (Smith, et al. 2001) data. A mosaic of the CTX DEMs produced for this work can be accessed on FigShare (<https://doi.org/10.6084/m9.figshare.19071560.v1>). Geospatial calculations and mapping were carried out with ESRI ArcMap software (v.10.3.1), including the ‘3D Analyst’ and ‘Spatial Analyst’ extensions (<https://www.esri.com/en-us/arcgis/products/arcgis-desktop/overview>).

## References

- Alemanno, G, V Orofino, and F Mancarella. 2018. "Global Map of Martian Fluvial Systems: Age and Total Eroded Volume Estimations." *Earth and Space Science* 5, no. 10: 560-577.
- Andrews-Hanna, J. C., M. T. Zuber, R. E. Arvidson, and S. M. Wiseman. 2010. "Early Mars Hydrology: Meridiani Playa Deposits and the Sedimentary Record of Arabia Terra." *Journal of Geophysical Research-Planets* 115 (Jun). <https://dx.doi.org/10.1029/2009je003485>.
- Baker, V. R., R. G. Strom, V. C. Gulick, J. S. Kargel, G. Komatsu, and V. S. Kale. 1991. "Ancient Oceans, Ice Sheets and the Hydrological Cycle on Mars." *Nature* 352, no. 6336 (Aug): 589-594. <https://dx.doi.org/10.1038/352589a0>.
- Cabrol, Nathalie A, and Edmond A Grin. 1999. "Distribution, Classification, and Ages of Martian Impact Crater Lakes." *Icarus* 142, no. 1: 160-172.
- Carr, M. H., and J. W. Head. 2003. "Oceans on Mars: An Assessment of the Observational Evidence and Possible Fate." *Journal of Geophysical Research-Planets* 108, no. E5 (May). <https://dx.doi.org/10.1029/2002je001963>.
- Carr, Michael H. 1995. "The Martian Drainage System and the Origin of Valley Networks and Fretted Channels." *Journal of Geophysical Research: Planets* 100, no. E4: 7479-7507.
- Christensen, P. R., B. Jakosky, H. H. Kieffer, M. C. Malin, H. Y. McSween, K. Nealson, G. L. Mehall, S. H. Silverman, S. Ferry, M. Caplinger, and M. Ravine. 2004. "The Thermal Emission Imaging System (Themis) for the Mars 2001 Odyssey Mission." *Space Science Reviews* 110, no. 1-2: 85-130. <https://dx.doi.org/10.1023/b:spac.0000021008.16305.94>.
- Clifford, S. M., and T. J. Parker. 2001. "The Evolution of the Martian Hy-

drosphere: Implications for the Fate of a Primordial Ocean and the Current State of the Northern Plains." *Icarus* 154, no. 1 (Nov): 40-79. <https://dx.doi.org/10.1006/icar.2001.6671>. Cook, Simon J, and Darrel A Swift. 2012. "Subglacial Basins: Their Origin and Importance in Glacial Systems and Landscapes." *Earth-Science Reviews* 115, no. 4: 332-372. Davis, JM, M Balme, PM Grindrod, RME Williams, and S Gupta. 2016. "Extensive Noachian Fluvial Systems in Arabia Terra: Implications for Early Martian Climate." *Geology* 44, no. 10: 847-850. Davis, Joel M, Sanjeev Gupta, Matthew Balme, Peter M Grindrod, Peter Fawdon, Zachary I Dickeson, and Rebecca ME Williams. 2019. "A Diverse Array of Fluvial Depositional Systems in Arabia Terra: Evidence for Mid-Noachian to Early Hesperian Rivers on Mars." *Journal of Geophysical Research: Planets* 124, no. 7: 1913-1934. Di Achille, G., and B. M. Hynek. 2010. "Ancient Ocean on Mars Supported by Global Distribution of Deltas and Valleys." *Nature Geoscience* 3, no. 7 (Jul): 459-463. <https://dx.doi.org/10.1038/ngeo891>. Di Achille, Gaetano, Brian M Hynek, and Mindi L Searls. 2009. "Positive Identification of Lake Strandlines in Shalbatana Vallis, Mars." *Geophysical Research Letters* 36, no. 14. Dickeson, Zachary I, and Joel M Davis. 2020. "Martian Oceans." *Astronomy & Geophysics* 61, no. 3: 3.11-3.17. Dickson, JL, MP Lamb, RME Williams, AT Hayden, and WW Fischer. 2020. "The Global Distribution of Depositional Rivers on Early Mars." *Geology*. Duran, Sergio, Tom J Coulthard, and Edwin RC Baynes. 2019. "Knickpoints in Martian Channels Indicate Past Ocean Levels." *Scientific reports* 9, no. 1: 1-6. Fairén, Alberto G, Alfonso F Davila, Darlene Lim, Nathan Bramall, Rosalba Bonaccorsi, Jhony Zavaleta, Esther R Uceda, Carol Stoker, Jacek Wierzchos, and James M Dohm. 2010. "Astrobiology through the Ages of Mars: The Study of Terrestrial Analogues to Understand the Habitability of Mars." *Astrobiology* 10, no. 8: 821-843. Fassett, Caleb I, and James W Head. 2008a. "The Timing of Martian Valley Network Activity: Constraints from Buffered Crater Counting." *Icarus* 195, no. 1: 61-89. ---. 2008b. "Valley Network-Fed, Open-Basin Lakes on Mars: Distribution and Implications for Noachian Surface and Subsurface Hydrology." *Icarus* 198, no. 1: 37-56. Favaro, EA, MR Balme, JM Davis, PM Grindrod, P Fawdon, AM Barrett, and SR Lewis. 2021. "The Aeolian Environment of the Landing Site for the Exomars Rosalind Franklin Rover in Oxia Planum, Mars." *Journal of Geophysical Research: Planets* 126, no. 4: 2020JE006723. Fawdon, Peter, Matthew R Balme, Joel M Davis, John Charles Bridges, Sanjeev Gupta, and Cathy Quantin-Nataf. 2021. "Rivers and Lakes in Western Arabia Terra: The Fluvial Catchment of the Exomars 2022 Rover Landing Site." *Journal of Geophysical Research: Planets*: e2021JE007045. Fawdon, Peter, Sanjeev Gupta, Joel M Davis, Nicholas H Warner, Jacob B Adler, Matthew R Balme, James F Bell III, Peter M Grindrod, and Elliot Sefton-Nash. 2018. "The Hypanis Valles Delta: The Last Highstand of a Sea on Early Mars?" *Earth and Planetary Science Letters* 500: 225-241. García-Arnay, Ángel, and Francisco Gutiérrez. 2020. "Reconstructing Paleolakes in Nepenthes Mensae, Mars, Using the Distribution of Putative Deltas, Coastal-Like Features, and Terrestrial Analogs." *Geomorphology*: 107129. Goudge, T. A., and C. I.

Fassett. 2018. "Incision of Licus Vallis, Mars, from Multiple Lake Overflow Floods." *Journal of Geophysical Research-Planets* 123, no. 2 (Feb): 405-420. <https://dx.doi.org/10.1002/2017je005438>. Goudge, T. A., C. I. Fassett, J. W. Head, J. F. Mustard, and K. L. Aureli. 2016. "Insights into Surface Runoff on Early Mars from Paleolake Basin Morphology and Stratigraphy." *Geology* 44, no. 6 (Jun): 419-422. <https://dx.doi.org/10.1130/g37734.1>. Goudge, Timothy A, Kelsey L Aureli, James W Head, Caleb I Fassett, and John F Mustard. 2015. "Classification and Analysis of Candidate Impact Crater-Hosted Closed-Basin Lakes on Mars." *Icarus* 260: 346-367. Goudge, Timothy A, James W Head, John F Mustard, and Caleb I Fassett. 2012. "An Analysis of Open-Basin Lake Deposits on Mars: Evidence for the Nature of Associated Lacustrine Deposits and Post-Lacustrine Modification Processes." *Icarus* 219, no. 1: 211-229. Head, James W, and David R Marchant. 2014. "The Climate History of Early Mars: Insights from the Antarctic McMurdo Dry Valleys Hydrologic System." *Antarctic Science* 26, no. 6: 774-800. Hynes, B. M., M. Beach, and M. R. T. Hoke. 2010. "Updated Global Map of Martian Valley Networks and Implications for Climate and Hydrologic Processes." *Journal of Geophysical Research-Planets* 115 (Sep). <https://dx.doi.org/10.1029/2009je003548>. Ireland, Richard L, Joseph Fairfield Poland, and Francis Stevenson Riley. 1984. *Land Subsidence in the San Joaquin Valley, California, as of 1980*. Vol. 437: US Government Printing Office. Kirk, Randolph L, Elpitha Howington-Kraus, Mark R Rosiek, Jeffery A Anderson, Brent A Archinal, Kris J Becker, DA Cook, Donna M Galuszka, Paul E Geissler, and Trent M Hare. 2008. "Ultra-high Resolution Topographic Mapping of Mars with MRO HiRISE Stereo Images: Meter-Scale Slopes of Candidate Phoenix Landing Sites." *Journal of Geophysical Research: Planets* 113, no. E3. Kite, Edwin S. 2019. "Geologic Constraints on Early Mars Climate." *Space Science Reviews* 215, no. 1: 10. Lamb, Michael P, William E Dietrich, Sarah M Aciego, Donald J DePaolo, and Michael Manga. 2008. "Formation of Box Canyon, Idaho, by Megaflood: Implications for Seepage Erosion on Earth and Mars." *Science* 320, no. 5879: 1067-1070. Langbein, Walter B, and Luna B Leopold. 1964. "Quasi-Equilibrium States in Channel Morphology." *American Journal of Science* 262, no. 6: 782-794. Malin, M. C., J. F. Bell, B. A. Cantor, M. A. Caplinger, W. M. Calvin, R. T. Clancy, K. S. Edgett, L. Edwards, R. M. Haberle, P. B. James, S. W. Lee, M. A. Ravine, P. C. Thomas, and M. J. Wolff. 2007. "Context Camera Investigation on Board the Mars Reconnaissance Orbiter." *Journal of Geophysical Research-Planets* 112, no. E5 (May). <https://dx.doi.org/10.1029/2006je002808>. Mangold, N., and V. Ansan. 2006. "Detailed Study of an Hydrological System of Valleys, a Delta and Lakes in the Southwest Thaumasia Region, Mars." *Icarus* 180, no. 1 (Jan): 75-87. <https://dx.doi.org/10.1016/j.icarus.2005.08.017>. McEwen, A. S., E. M. Eliason, J. W. Bergstrom, N. T. Bridges, C. J. Hansen, W. A. Delamere, J. A. Grant, V. C. Gulick, K. E. Herkenhoff, L. Keszthelyi, R. L. Kirk, M. T. Mellon, S. W. Squyres, N. Thomas, and C. M. Weitz. 2007. "Mars Reconnaissance Orbiter's High Resolution Imaging Science Experiment (HiRISE)." *Journal of Geophysical Research-Planets* 112, no. E5 (May). <https://dx.doi.org/10.1029/2005je002605>. McNeil, Joseph D., Peter

Fawdon, Matthew R. Balme, and Angela L. Coe. 2021. "Morphology, Morphometry and Distribution of Isolated Landforms in Southern Chryse Planitia, Mars." *Journal of Geophysical Research: Planets* 126, no. 5: e2020JE006775. <https://dx.doi.org/https://doi.org/10.1029/2020JE006775>. Milliken, RE, Ryan C Ewing, WW Fischer, and J Hurowitz. 2014. "Wind-Blown Sandstones Cemented by Sulfate and Clay Minerals in Gale Crater, Mars." *Geophysical Research Letters* 41, no. 4: 1149-1154. Milliken, RE, JP Grotzinger, and BJ Thomson. 2010. "Paleoclimate of Mars as Captured by the Stratigraphic Record in Gale Crater." *Geophysical Research Letters* 37, no. 4. Neukum, Gerhard, and Ralf Jaumann. 2004. *Hrsc: The High Resolution Stereo Camera of Mars Express*. Vol. 1240. *Mars Express: The Scientific Payload*. Palumbo, Ashley M, James W Head, and Robin D Wordsworth. 2018. "Late Noachian Icy Highlands Climate Model: Exploring the Possibility of Transient Melting and Fluvial/Lacustrine Activity through Peak Annual and Seasonal Temperatures." *Icarus* 300: 261-286. Parker, T. J., R. S. Saunders, and D. M. Schneeberger. 1989. "Transitional Morphology in West Deuteronilus Mensae, Mars - Implications for Modification of the Lowland Upland Boundary." *Icarus* 82, no. 1 (Nov): 111-145. [https://dx.doi.org/10.1016/0019-1035\(89\)90027-4](https://dx.doi.org/10.1016/0019-1035(89)90027-4). Parker, Timothy J, Dale M Schneeberger, David C Pieri, and R Stephen Saunders. 1986. *Geomorphic Evidence for Ancient Seas on Mars*. Vol. 599. *Mars: Evolution of its Climate and Atmosphere*. Rivera-Hernández, Frances, and Marisa C Palucis. 2019. "Do Deltas Along the Crustal Dichotomy Boundary of Mars in the Gale Crater Region Record a Northern Ocean?" *Geophysical Research Letters* 46, no. 15: 8689-8699. Rosenberg, Elliott N, and James W Head. 2015. "Late Noachian Fluvial Erosion on Mars: Cumulative Water Volumes Required to Carve the Valley Networks and Grain Size of Bed-Sediment." *Planetary and Space Science* 117: 429-435. Salese, Francesco, Gaetano Di Achille, Adrian Neesemann, Gian Gabriele Ori, and Ernst Hauber. 2016. "Hydrological and Sedimentary Analyses of Well-Preserved Paleofluvial-Paleolacustrine Systems at Moa Valles, Mars." *Journal of Geophysical Research: Planets* 121, no. 2: 194-232. Salese, Francesco, Maarten G Kleinhans, Nicolas Mangold, Veronique Ansan, William McMahon, Tjalling de Haas, and Gilles Dromart. 2020. "Estimated Minimum Life Span of the Jezero Fluvial Delta (Mars)." *Astrobiology* 20, no. 8: 977-993. Salese, Francesco, Monica Pondrelli, Alicia Neeseman, Gene Schmidt, and Gian Gabriele Ori. 2019. "Geological Evidence of Planet-Wide Groundwater System on Mars." *Journal of Geophysical Research: Planets* 124, no. 2: 374-395. Sato, Hiroyuki, Kei Kurita, and David Baratoux. 2010. "The Formation of Floor-Fractured Craters in Xanthe Terra." *Icarus* 207, no. 1: 248-264. Sholes, Steven F., Zachary I. Dickeson, David R. Montgomery, and David C. Catling. 2021. "Where Are Mars' Hypothesized Ocean Shorelines? Large Lateral and Topographic Offsets between Different Versions of Paleoshoreline Maps." *Journal of Geophysical Research: Planets* 126, no. 5: e2020JE006486. <https://dx.doi.org/https://doi.org/10.1029/2020JE006486>. Smith, D. E., M. T. Zuber, H. V. Frey, J. B. Garvin, J. W. Head, D. O. Muhleman, G. H. Pettengill, R. J. Phillips, S. C. Solomon, H. J. Zwally, W. B. Banerdt, T. C. Duxbury, M. P. Golombek, F. G. Lemoine, G. A. Neumann, D. D. Rowlands,

O. Aharonson, P. G. Ford, A. B. Ivanov, C. L. Johnson, P. J. McGovern, J. B. Abshire, R. S. Afzal, and X. L. Sun. 2001. "Mars Orbiter Laser Altimeter: Experiment Summary after the First Year of Global Mapping of Mars." *Journal of Geophysical Research-Planets* 106, no. E10 (Oct): 23689-23722. <https://dx.doi.org/10.1029/2000je001364>. Tanaka, K. L., J. A. Skinner, T. M. Hare, T. Joyal, and A. Wenker. 2003. "Resurfacing History of the Northern Plains of Mars Based on Geologic Mapping of Mars Global Surveyor Data." *Journal of Geophysical Research-Planets* 108, no. E4 (Apr). <https://dx.doi.org/10.1029/2002je001908>. Tanaka, KL, JA Skinner, JM Dohm, RP Irwin, EJ Kolb, CM Fortezzo, T Platz, GG Michael, and TM Hare. 2014. "Geologic Map of Mars, Scientific Investigations Map 3292." *US Geol. Sur., doi i* 10. Watters, Thomas R, Patrick J McGovern, and Rossman P Irwin Iii. 2007. "Hemispheres Apart: The Crustal Dichotomy on Mars." *Annu. Rev. Earth Planet. Sci.* 35: 621-652. Webb, V. E. 2004. "Putative Shorelines in Northern Arabia Terra, Mars." *Journal of Geophysical Research-Planets* 109, no. E9 (Sep). <https://dx.doi.org/10.1029/2003je002205>. Williams, Rebecca ME, Jeffrey E Moersch, and Robin L Fergason. 2018. "Thermophysical Properties of Martian Fluvial Sinuous Ridges: Inferences on "Inverted Channel" Induration Agent." *Earth and Space Science* 5, no. 9: 516-528. Wilson, S. A., A. D. Howard, J. M. Moore, and J. A. Grant. 2016. "A Cold-Wet Middle-Latitude Environment on Mars During the Hesperian-Amazonian Transition: Evidence from Northern Arabia Valleys and Paleolakes." *Journal of Geophysical Research-Planets* 121, no. 9 (Sep): 1667-1694. <https://dx.doi.org/10.1002/2016je005052>.